PRAMANA
— journal of
physics

© Indian Academy of Sciences

Vol. 62, No. 4
April 2004
pp. 827–839

Shape change in Hf, W and Os-isotopes: A non-relativistic Hartree–Fock versus relativistic Hartree approximation

Z NAIK[a], B K SHARMA[a], T K JHA[b], P ARUMUGAM[a] and S K PATRA[a]
[a]Institute of Physics, Sachivalaya Marg, Bhubaneswar 751 005, India
[b]P.G. Department of Physics, Sambalpur University, Jyoti Vihar, Burla 768 019, India
E-mail: patra@iopb.res.in

MS received 27 August 2003; revised 13 November 2003; accepted 3 January 2004

Abstract. We have investigated the ground-state structures of even–even Hf, W and Os isotopes within the framework of a deformed non-relativistic Hartree–Fock and a relativistic mean field formalism. A majority of the nuclei are predicted to be prolate in shape in the relativistic calculations. On the other hand, contrary to the relativistic results, we predict a shape change in a cyclic order in the non-relativistic calculations. However, in both the cases, the magnitude of the quadrupole deformation parameter agrees well with the experimental data. We also evaluated the hexadecapole deformation parameter for Hf, W and Os isotopes and irrespective of the shape change in quadrupole moments, we find a cyclic change in hexadecapole shape from positive to negative and vice versa in both the relativistic and non-relativistic formalisms.

Keywords. Binding energies; quadrupole deformations; drip-line nuclei; relativistic mean field theory; non-relativistic Hartree–Fock.

PACS Nos 21.10.Dr; 21.10.Tg; 21.60.-n; 21.60.Fw

1. Introduction

In the rare-earth region the change of shape from prolate to oblate and vice versa is a common phenomenon [1]. This shape change of a nucleus in an isotopic chain has been studied using relativistic [2] and non-relativistic [3] models. For quite a long time, the change of quadrupole moment from oblate to prolate while going from lighter to heavier isotopes has been reported theoretically [4] and experimentally [5,6]. The change of shape of rare-earth nuclei from oblate to prolate deformation while going from the neutron-deficient to the neutron-rich side has been studied using a self-consistent non-relativistic Hartree–Fock–Bogoliubov (NHFB) approach in a pairing plus quadrupole plus hexadecapole model [7]. Using various formalisms, the quadrupole and hexadecapole moments for rare-earth nuclei have been investigated theoretically [8] and measured experimentally [9].

To explain this shape change, a large number of theoretical calculations are reported [10,11]. Due to the availability of the radioactive beam in various laboratories, it is now possible to study the structural properties of light nuclei near the proton and neutron drip-lines. However, it is not so easy experimentally to reach the drip-line in the medium and heavy mass region of the mass table. In the present decade the structural investigation of drip-line nuclei is an interesting study. For light nuclei the existence of halo is a well-established discovery. On the other hand the shape change in an isotopic series is an enthusiastic analysis in the rare-earth region of the periodic table. In this context, we choose hafnium (Hf), tungsten (W) and osmium (Os) nuclei as the representative elements of this mass region. We used two most powerful techniques, viz., the deformed non-relativistic Hartree–Fock (NHF) and relativistic mean field (RMF) theories, to analyse the structures of nuclei starting from the proton to the neutron drip-lines. Here, the quadrupole and hexadecapole deformation parameters β_2 and β_4, the binding energies for both the ground and excited states and the potential energy surfaces (PES) for some of the selected nuclei are calculated and analysed with a view to look for the shape change.

In our earlier publications [10,11] we have shown that the hexadecapole shape change occurs in ytterbium isotopes with increasing mass number. There we have shown that a group of neutron orbitals with large negative (or positive) hexadecapole moments present together near the transition point and are responsible for the hexadecapole shape change. We repeated the calculations in an extended manner and reported the results for Yb and Hf in ref. [11] with various relativistic parameter sets. Here we will re-visit the region and will perform the calculations with recently developed relativistic parameter sets (NL3 and NL-RA1) and will compare the results with NHF calculations using a surface delta interaction.

For the last several decades, the NHF formalism is a very useful method to determine the nuclear structures. Using the NHF method, one can calculate the quadrupole and other higher order multipole deformation in a satisfactory accuracy. Application of angular momentum projection (AMP) project the good angular momentum J from the intrinsic states and gives the correct ground and excited states. On the other hand, in the last two decades, the RMF model is known to be a very powerful tool to explain the properties of finite nuclei and infinite nuclear matter [12–14]. The RMF method has the advantage that, with proper relativistic kinematics and the mesons and their properties already known or fixed from the properties of a few nuclei [12,15,16], the method gives excellent results for binding energies, root mean square (rms) radii, quadrupole and hexadecapole deformations and other nuclear properties, not only of spherical, but also of deformed nuclei. One of the most attractive features of the RMF formalism is that the spin-orbit strength and associated nuclear shell structure automatically arise from meson–nucleon interaction [17,18].

The paper is organised as follows: In §2 we outline the essential formalism for the non-relativistic Hartree–Fock and relativistic Hartree formalisms. The results and their discussions for Hf, W and Os isotopes are given in §3. In this section, we look for the quadrupole and hexadecapole shape change and the coexistence nature of prolate and oblate structures in some of the cases. Finally, §4 contains summary and conclusions.

2. Formalisms

2.1 *Non-relativistic Hartree–Fock*

Theoretically, the band structure of the Nilsson orbit $[Nn_3\Lambda]\Omega^\pi$, is studied with a well-known microscopic model, i.e., deformed Hartree–Fock and angular momentum projection [19,20]. In this calculation, axial symmetry of the Hartree–Fock field is assumed. The nuclear Hamiltonian consists of single-particle and residual two-body interaction terms and is defined as

$$H = \epsilon + V. \tag{1}$$

(Here, schematically ϵ stands for single-particle energies and V stands for two-body interactions *pp*, *pn*, *nn*). The residual two-body interaction in the present case is taken to be the surface delta residual interaction with interaction strength $F_{pp} = F_{np} = F_{nn} = 0.3$ MeV. This is a reasonable interaction which gives the deformation properties in these mass region [21] quite well. The deformed NHF orbits are calculated with a spherical closed shell core of $Z = 50$ and $N = 82$ (^{132}Sn is taken as the spherical core). The model space with respective single-particle energies used for the NHF orbits and angular momentum projection spectra calculation are given in table 1.

Deformed NHF orbit is in general a superposition of various j states. An intrinsic state $|\phi_K\rangle$ is a Slater determinant of such deformed orbits and is obtained from the NHF configuration by appropriate particle–hole arrangement near the proton and neutron Fermi surfaces. A given intrinsic state $|\phi_K\rangle$ does not have a unique angular momentum quantum number and is a superposition of various J states (intrinsic states are states of good K but not of good J) and is defined as

$$|\phi_K\rangle = \sum_J C_K^J |\Psi_{JK}\rangle, \tag{2}$$

where C is the amplitude of the state of angular momentum J.

The nuclear Hamiltonian is rotationally invariant. Here rotational symmetry is restored by angular momentum (J) projection. By angular momentum projection from these intrinsic states the spectra and other spectroscopic properties (transition rates) can be obtained. The angular momentum projection operator is

$$P_K^{JM} = \frac{2J+1}{8\pi^2} \int \mathrm{d}\Omega \; D_{MK}^{J*}(\Omega) R(\Omega), \tag{3}$$

Table 1. Single-particle energies of protons and neutrons.

Proton	$g_{7/2}$	$d_{5/2}$	$s_{1/2}$	$d_{3/2}$	$h_{11/2}$	$h_{9/2}$
(MeV)	0	0.731	3.654	3.288	1.705	7.1
Neutron	$f_{7/2}$	$p_{3/2}$	$f_{5/2}$	$h_{9/2}$	$p_{1/2}$	$i_{13/2}$
(MeV)	0	2.974	3.432	0.686	4.462	1.487

where $R(\Omega)$ is the rotational operator and Ω stands for the Euler angles. For intrinsic states with axial symmetry, two of the Euler angles α, γ are integrated and we are left with the integrals for the kernels for the Euler angle β.

The matrix element of the Hamiltonian between projected states of angular momentum J obtained from intrinsic states ϕ_{K_1} and ϕ_{K_2} is

$$H^J_{K_1K_2} = \frac{2J+1}{2}\frac{1}{(N^J_{K_1K_1}N^J_{K_2K_2})^{1/2}} \times \int_0^\pi \mathrm{d}\beta \sin\beta d^J_{K_1K_2}(\beta)\langle\phi_{K_1}|H\mathrm{e}^{-i\beta J_y}|\phi_{K_2}\rangle, \tag{4}$$

where

$$N^J_{K_1K_2} = \frac{2J+1}{2}\int_0^\pi \mathrm{d}\beta \sin\beta d^J_{K_1K_2}(\beta)\langle\phi_{K_1}|\mathrm{e}^{-i\beta J_y}|\phi_{K_2}\rangle \tag{5}$$

is the amplitude overlap for angular momentum J.

In our calculations, the effective charges of $1.7e$ for protons and $0.7e$ for neutrons are used to calculate β_2 and β_4 values.

We have performed deformed Hartree–Fock calculations for a series of Hf, W and Os isotopes. Then to see the lowering in energy of the intrinsic binding we carried out the angular momentum projection [20] for some of the selected nuclei having various deformations. A deformed intrinsic state is a superposition of various angular momentum states, and after angular momentum projection the ground state is lowered in energy as compared to the intrinsic state. This lowering is large for configurations with large β_2 values. For the $K = 0$ intrinsic state

$$|\Phi_{\mathrm{intr}}\rangle = \sum_J C_J \Psi_{J0}.$$

Then,

$$E_{\mathrm{intr}} = \langle\Phi_{\mathrm{intr}}|H|\Phi_{\mathrm{intr}}\rangle = \sum_J |C_J|^2 E_J,$$

giving the ground state energy as

$$E_0 = \frac{1}{C_0^2}\Big[E_{\mathrm{intr}} - \sum_J{}' |C_J|^2 E_J\Big].$$

Here, the primed summation means that it does not include $J = 0$. Apparently, E_{intr} can be identified with E_0 only for spherical solutions (containing only 0^+ state). However, in the present work angular momentum projection is considered for some selected nuclei to realise an estimation of the real ground state binding energy. In other words, we are concerned here only with normal deformed state, such as the lowering in binding energies is estimated to be about less than two MeV (will be discussed later). And also, we are concerned here only with bulk properties, such as the binding energies, nuclear deformations and the average properties of the intrinsic states and not with the spectroscopy of the bands in the studied nuclei.

2.2 *Relativistic Hartree approximation*

The relativistic mean field approach is well-known and its theory can be found in refs [15–18,22,23]. We start with the relativistic Lagrangian density for a nucleon–meson many-body system:

$$\begin{aligned}\mathcal{L} = {} & \overline{\psi_i}\{i\gamma^\mu\partial_\mu - M\}\psi_i + \frac{1}{2}\partial^\mu\sigma\partial_\mu\sigma - \frac{1}{2}m_\sigma^2\sigma^2 - \frac{1}{3}g_2\sigma^3 - \frac{1}{4}g_3\sigma^4 \\ & - g_s\overline{\psi_i}\psi_i\sigma - \frac{1}{4}\Omega^{\mu\nu}\Omega_{\mu\nu} + \frac{1}{2}m_w^2V^\mu V_\mu - g_w\overline{\psi}_i\gamma^\mu\psi_iV_\mu \\ & - \frac{1}{4}\vec{B}^{\mu\nu}\cdot\vec{B}_{\mu\nu} + \frac{1}{2}m_\rho^2\vec{R}^\mu\cdot\vec{R}_\mu - g_\rho\overline{\psi}_i\gamma^\mu\vec{\tau}\psi_i\cdot\vec{R^\mu} \\ & - \frac{1}{4}F^{\mu\nu}F_{\mu\nu} - e\overline{\psi}_i\gamma^\mu\frac{(1-\tau_{3i})}{2}\psi_iA_\mu. \end{aligned} \tag{6}$$

The field for the σ meson is denoted by σ, that for the ω meson by V_μ and for the isovector ρ meson by $\vec{R}_\mu$. A^μ denotes the electromagnetic field. The ψ_i are the Dirac spinors for the nucleons whose third component of isospin is denoted by τ_{3i}. Here g_s, g_w, g_ρ and $(e^2/4\pi) = (1/137)$ are the coupling constants for σ, ω, ρ mesons and photon, respectively. g_2, g_3 and c_3 are the parameters for the non-linear terms of σ and ω mesons. M is the mass of the nucleon and m_σ, m_ω and m_ρ are the masses of the σ, ω and ρ mesons, respectively. $\Omega^{\mu\nu}$, $\vec{B}^{\mu\nu}$ and $F^{\mu\nu}$ are the field tensors for the V^μ, $\vec{R}^\mu$ and the photon fields, respectively [15].

From the relativistic Lagrangian we get the field equations for the nucleons and mesons. These equations are solved by expanding the upper and lower components of Dirac spinors and the boson fields in a deformed harmonic oscillator basis with an initial deformation. The set of coupled equations is solved numerically by a self-consistent iteration method. The centre-of-mass motion is estimated by the usual harmonic oscillator formula $E_{\text{c.m.}} = \frac{3}{4}(41A^{-1/3})$. The quadrupole ($\beta_2$) and hexadecapole deformation parameter (β_4) are evaluated from the resulting quadrupole (Q_2) and hexadecapole (Q_4) moment [15] using the formula

$$Q = Q_n + Q_p = \sqrt{\frac{9}{5\pi}}AR^2\beta_2, \tag{7}$$

and the hexadecapole moment obtained from the expression

$$Q_4^{n,p} = \langle r^4Y_{40}(\theta)\rangle_{n,p}, \tag{8}$$

where $R = 1.2A^{1/3}$. The β_4 value is obtained from the hexadecapole moment through the formula $Q_4 = (3/4\pi)AR^4\beta_4$. The total binding energy of the system is

$$E_{\text{total}} = E_{\text{part}} + E_\sigma + E_\omega + E_\rho + E_{\text{c}} + E_{\text{pair}} + E_{\text{c.m.}}, \tag{9}$$

where E_{part} is the sum of the single-particle energies of the nucleons and E_σ, E_ω, E_ρ, E_{c} and E_{pair} are the contributions of the mesons fields, the Coulomb field and the pairing energy, respectively. For the open shell nuclei the effect of pairing interactions is added in the BCS formalism. The pairing gaps for proton Δ_p and neutron Δ_n are calculated from the relations [24]:

$$\Delta_p = rb_s Z^{-1/3} \mathrm{e}^{(sI - tI^2)},$$
$$\Delta_n = rb_s N^{-1/3} \mathrm{e}^{-(sI + tI^2)}, \tag{10}$$

where $r = 5.72$ MeV, $s = 0.118$, $t = 8.12$, $b_s = 1$ and $I = (N - Z)/(N + Z)$. In the present calculations, we will use $N_\mathrm{F} = N_\mathrm{B} = 12$ oscillator shells as the expansion basis for the fermion and boson fields, which is reasonably a good model space for this mass region to estimate the gross nuclear bulk properties.

3. Results and discussions

In this section, we discuss the results of our non-relativistic Hartree–Fock with surface-δ-interaction and the results obtained by relativistic mean field calculations. NL3, the most successful parameter set known till date [25,26] and the recent NL-RA1 [27] parameter sets are employed for the present RMF calculations. To show the accuracy of our results with the experimental data, we display our results in table 2 for some Hf, W and Os isotopes, where experimental data are available. This table also gives a quantitative comparison between the superiority of NL3 and NL-RA1 sets. In table 2, we notice that the calculated binding energies and quadrupole deformation parameters β_2, for both the sets, are quite close to the experimental values [28,29]. Also, interesting enough, both the parameter sets give almost similar results. A further inspection of table 2 shows that NL-RA1 is relatively better than NL3 for predicting the experimental binding energies. The quadrupole deformation parameter β_2 is also given in the table. From the table, it is clear that the value of β_2 is almost similar both in NL3 and NL-RA1 sets. Again the quadrupole deformation parameters obtained by RMF formalism agree excellently well with the NHF calculations. When we compare our calculated results with the experimental deformation parameters, wherever possible, we get remarkably close with the experimental data. Note that the evaluation of quadrupole deformation parameter β_2 from the experimental B(E2)-value [29] gives the absolute β_2 and hence is unable to determine its sign. Thus, a comparison of the calculated β_2 with experimental β_2 is limited in this respect.

The AMP results for some of the selected nuclei are displayed in table 3. We noticed an energy lowering of about 1–2 MeV from the binding energy of the intrinsic states. The angular momentum projection in the framework of RMF formalism is beyond the scope of the paper. However, the AMP results obtained by the non-relativistic formalism give an idea about the energy lowering (depending on the quadrupole deformation) for this mass region.

In figures 1a, 1b and 1c, the difference ΔE of the binding energies between the intrinsic ground state and the first intrinsic excited state, with the pairing interactions included (in RMF), is shown for Hf, W and Os isotopes. The ΔE of non-relativistic Hartree–Fock energy is also given in the same figure. (From here onwards we refer intrinsic ground state as the ground state and the intrinsic excited state as simply excited state.) It is clear from figure 1 that most of the ground state energy is maximum for the prolate shape. This means, apart from a few isotopes, most nuclei in Hf, W and Os series are prolate in shape in their ground state configurations in the relativistic mean field calculations. Contrary to the RMF results, we find a shape change from prolate to oblate and again

Table 2. The ground state binding energy BE and the quadrupole deformation parameter β_2 for some Hf, W and Os isotopes obtained by the two approaches NHF (surface-δ) and RMF (NL-RA1 and NL3). In case of NHF the HF energy is calculated with ^{132}Sn as core. The experimental (or extrapolated) values are also given [29]. The binding energy is in MeV.

	BE		HF energy	BE	β_2			
Nuclei	NL-RA1	NL3	Surface-δ	Expt.	NL-RA1	NL3	Surface-δ	Expt.
^{166}Hf	1337.0	1339.7	124.1	1337.3	0.299	0.294	0.249	0.249
^{168}Hf	1355.0	1357.5	141.8	1355.0	0.325	0.324	0.259	0.274
^{170}Hf	1371.7	1374.4	159.4	1372.0	0.332	0.334	0.267	0.296
^{172}Hf	1387.5	1390.4	177.3	1388.3	0.330	0.336	0.276	0.274
^{174}Hf	1403.1	1405.8	196.2	1404.0	0.316	0.324	−0.330	0.284
^{176}Hf	1418.2	1420.8	216.6	1418.8	0.303	0.307	−0.337	0.295
^{178}Hf	1432.2	1434.8	234.7	1432.8	0.293	0.295	−0.340	0.280
^{180}Hf	1445.5	1447.9	250.6	1446.3	0.284	0.286	0.278	0.273
^{168}W	1342.8	1345.8	130.8	1342.9	0.302	0.212	0.301	0.232
^{170}W	1361.9	1364.8	149.7	1361.5	0.322	0.321	0.234	0.242
^{172}W	1379.8	1382.8	168.2	1379.4	0.329	0.332	0.241	0.309
^{180}W	1444.5	1447.1	249.0	1444.6	0.287	0.290	−0.318	0.252
^{182}W	1459.1	1461.6	266.1	1459.3	0.273	0.275	−0.313	0.249
^{184}W	1472.5	1475.1	282.1	1473.0	0.260	0.262	−0.303	0.235
^{186}W	1485.2	1487.9	299.5	1485.9	0.245	0.247	0.224	0.224
^{182}Os	1454.7	1457.5	262.7	1454.1	0.301	0.304	−0.287	0.233
^{184}Os	1470.0	1472.7	281.0	1470.0	0.285	0.287	−0.283	0.212
^{186}Os	1483.8	1486.7	298.6	1484.8	0.268	0.269	0.273	0.200
^{188}Os	1497.0	1499.0	316.3	1499.1	0.245	0.246	0.192	0.186
^{190}Os	1510.4	1513.2	336.2	1512.8	0.206	0.206	0.187	0.176
^{192}Os	1523.6	1526.4	355.3	1526.1	0.180	0.178	0.172	0.165

Table 3. The energy lowering in non-relativistic angular momentum projection for some of the selected W isotopes. Note that the ground state quadrupole and hexadecapole deformation remain unchanged in the angular momentum projection.

	Before projection		After projection	
Nuclei	BE	β_2	BE	Lowering
^{164}W	93.825	0.19139	94.995	1.17
^{174}W	187.143	0.25143	188.497	1.35
^{184}W	281.696	0.23599	283.810	2.11
^{190}W	335.118	0.20337	337.335	2.21

from oblate to prolate in the non-relativistic Hartree–Fock approach. Further, we notice a shape coexistence region with NL-RA1 and NL3 sets at mass number $A \approx 154, 198$ for all the three isotopic series (Hf, W and Os) considered here. In

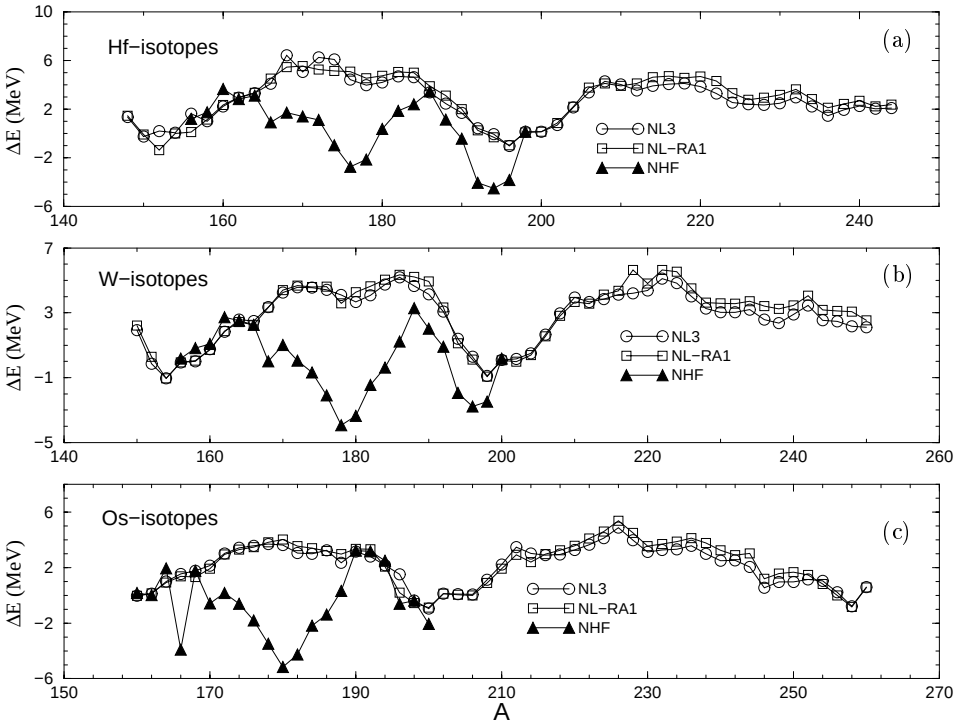

Figure 1. Binding energy difference between the intrinsic ground state and the first intrinsic excited state.

the NHF calculations, the shape coexistence nuclei are ^{180,190,198}Hf, ^{158,168,172,202}W and ^{160,162,172,188}Os. We considered here the shape coexistence cases if the intrinsic binding energy difference between the ground and excited state is less than 1 MeV. In all the three cases, we find similar trends of the ΔE values.

To get a realization about the barrier between the ground and excited states, the potential energy surfaces (PES) are calculated. A constrained calculation is carried out [30], where, instead of minimizing $\langle H_0 \rangle$, we have minimized $\langle H - \lambda Q \rangle$, with λ as a Lagrange multiplier and Q the quadrupole moment. There are many theoretical calculations available in the literature for calculating the potential energy surface (PES) diagram and to analyse the different structures of nuclei in different mass regions of the periodic table [31,32]. Wood *et al* [31] pointed out that in many cases the minima in 0-quasiparticle PES, even if they are very shallow and separated by very low energy barriers, correspond to well-defined states. They showed that, even the structures which do not correspond to a local minimum in PES may be closely related to the physical state of the nucleus, whose energy can be successfully extracted by removing spurious interactions with excited configurations. The number of particles occupying the single-particle intruder orbits can be treated as an additional quantum number. These observations suggest that a flat PES does not automatically lead to large fluctuations of shape. On the contrary, the nucleus may still be fairly rigid, the shape being restored not by a large energy barrier but by

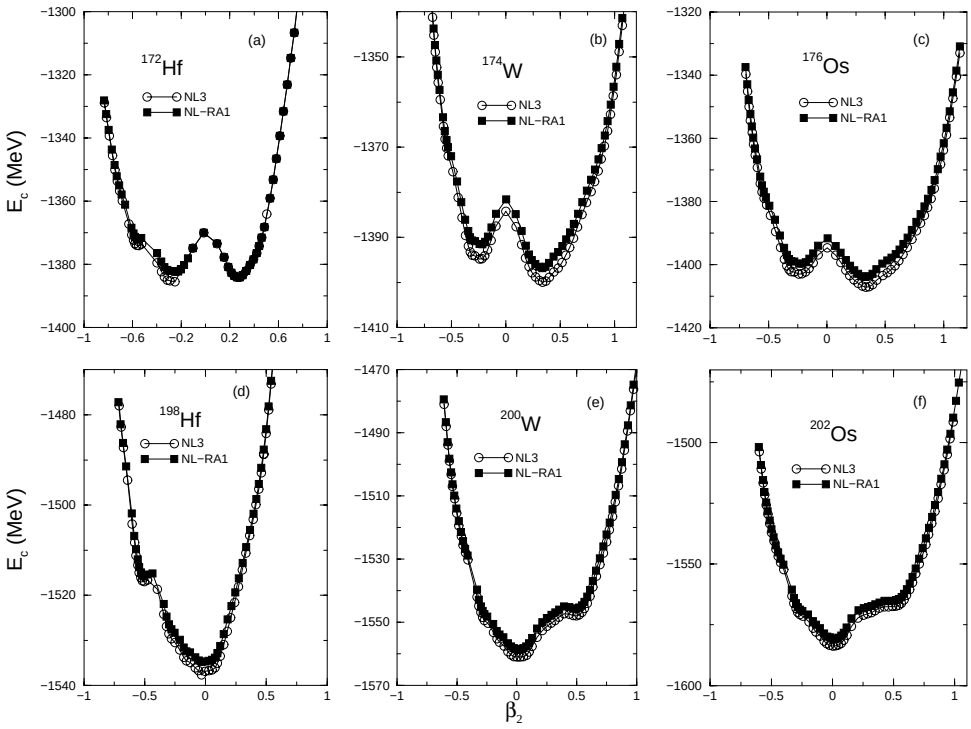

Figure 2. The potential energy surface diagram for ^{172,198}Hf, ^{174,200}W and ^{176,202}Os.

profound structural differences between different minima [31,32]. It is to be noted here that, in nature, the triaxial degree of freedom is very important but triaxiality destroys the possibility of many isomers and allows a large amount of configuration mixing. In this way the violation of axial symmetry is possible [33–35]. Recently exotic shapes (non-axial, with octupole deformations) and shape coexistence in $N = Z$ proton-rich nuclei from ^{64}Ge to ^{84}Mo by symmetry-unrestricted Skyrme–Hartree–Fock–Bogoliubov (Skyrme–HFB) methods have been reported [36], where the PES are calculated in constrained Skyrme–HFB approach. However, in the present calculation the triaxial degree of freedom is beyond the scope of our work. Therefore, we have restricted our calculation to an axially deformed RMF calculation only [8,37–39].

The PES is plotted in figures 2a–f for ^{172,198}Hf, ^{174,200}W and ^{176,202}Os, the most deformed and the least deformed nuclei in the investigated series. Here the binding energy is shown as a function of the quadrupole deformation parameter β_2. We find two distinct minima for ^{172}Hf, ^{174}W and ^{176}Os at quadrupole deformation $\beta_2 \approx -0.25$ and $\beta_2 \approx 0.35$, separated by a potential barrier of about 15 MeV. The PES is shown in figures 2d–f for ^{198}Hf, ^{200}W and ^{202}Os the least deformed nuclei in the series. In this case, an absolute minima is predicted at zero deformation in each of the nuclei. A very shallow minimum is also shown at very highly excited

position, which cannot be an excited state due to the extremely shallow structure in the PES diagrams.

The variation of the quadrupole deformation parameter β_2 with mass number A for the two cases (relativistic and non-relativistic) are shown in figures 3a–c. For comparison the result obtained by finite range droplet model (FRDM) is also displayed in the same figure. We notice that the pattern of the deformation is almost similar for all the three isotopic series. As we have discussed in the binding energy differences between prolate and oblate solutions, here we find positive β_2 for most of the nuclei in the RMF calculations. We obtain oblate ground state structures for very few cases in the RMF calculations. This means, in RMF, ^{150,152,196,198}Hf, ^{152,154,198}W and ^{198,200}Os are oblate in shape. We find a cyclic change in deformation for the NHF calculations, which means, in NHF prediction, $^{174-186,196-200}$Os are oblate in shape. From figures 3a–c, it can be seen clearly that the quadrupole deformation obtained by RMF matches with the FRDM calculations more closely than with the results predicted by NHF. This pattern of results follow for all the three isotopes (Hf, W and Os) considered in the present calculations.

It is worth mentioning that the non-relativistic Hartree–Fock calculation is based on the surface-δ-interaction. It is a crude interaction and in general predicts the overall properties of the nuclei. For the large dimension of the model space, the calculation is done by taking ^{132}Sn as an inert core. By virtue of this, some times we are missing the detailed internal structure of the nucleus. As a result, the prediction of NHF model differs in many cases, as it occurs in the present calculations. Another assumption made in the present NHF calculations is the fixed single-particle energy levels (given in table 1) used for initial guess for all the nuclei considered. It is well-known that the distribution of the single-particle levels change as we move from one nucleus to the other [40]. In principle the initial single-particle energies should not make much difference in results. However, in real practice, the HF energy slightly depends on the initial input of the single-particle energies. Consequently the difference between energies of the prolate and oblate configurations fluctuate. In general, in our calculations, the magnitude of the quadrupole deformation parameters in NHF solution agree well with the RMF prediction, if we fix the deformation to be either prolate or oblate. The discrepancy of NHF results with other theories may be attributed to the above-mentioned reasons. A much more realistic interaction as reported in ref. [41], in addition to a larger model space is essential to get better results in NHF formalism. Work in this direction is in progress [42].

One of the interesting physical quantity in nuclear structure is the hexadecapole deformation parameter β_4. In a simple calculation it has been shown in refs [43,44] that the sign of β_4 changes with mass A in an isotopic chain. Also in the framework of a relativistic microscopic calculations, in our earlier works, in the rare-earth region, we have shown that the sign of the hexadecapole deformation changes with increase of mass number [10,11]. This is just like an oscillation from positive to negative and vice versa (figures 3d–f). Here we observed the oscillation of β_4 with increase in mass number. It is to be noted that irrespective of the prolate or oblate ground state, we see a cyclic hexadecapole shape change for all the three Hf, W and Os isotopes. In general, both the RMF and NHF results agree with each other as well as with the prediction of FRDM calculations.

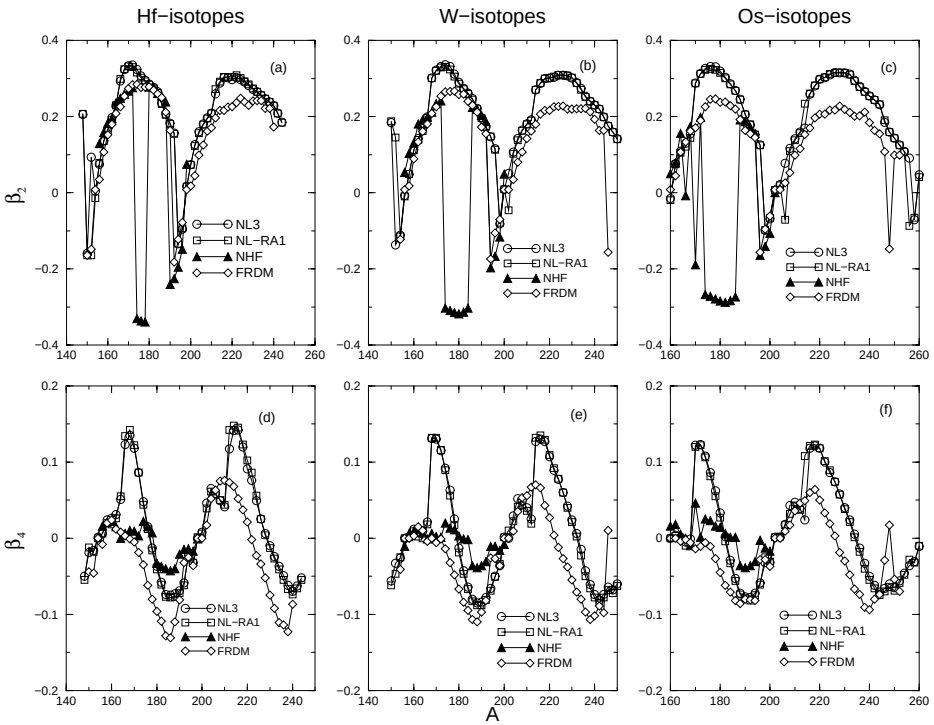

Figure 3. The ground state quadrupole deformation parameter β_2 and the hexadecapole deformation parameter (β_4) as a function of mass number A for non-relativistic Hartree–Fock with surface-δ-interaction and for relativistic Hartree with NL3 and NL-RA1 forces.

4. Summary and conclusions

In the present paper, we calculate the binding energies and the relative binding energy with RMF and NHF formalisms, respectively. We predicted the ground state configurations taking into account the maximum ground state binding energy (in RMF) or the maximum relative binding (in NHF). In the present paper, we performed angular momentum projection for some of the selected nuclei for the normal deformed states and found that the lowering in ground state binding energy is less than 2 MeV. Since our motivation was on the ground state bulk properties, we did not have to be concerned about the spectroscopy of the nuclei and we did not perform angular momentum projection for the whole isotopic series. We then evaluated the quadrupole and hexadecapole deformation parameters in the isotopic chain of Hf, W and Os nuclei. A few isotopes are predicted to be oblate in their ground state in the framework of RMF predictions. However, we find a cyclic change of quadrupole deformation parameter in an isotopic series in the non-relativistic Hartree–Fock model. The trends of RMF calculations are found to be closer to the macro–microscopic finite range droplet model. For the case of hexadecapole deformation parameter we find a cyclic change of sign from negative to positive

and again from positive to negative irrespective of the ground state quadrupole moments. This change of sign in β_4 is found to be model as well as parameter independent in our calculations and agree well with the FRDM predictions.

References

[1] S K Patra and P K Panda, *Phys. Rev.* **C47**, 1514 (1993)
[2] S K Patra, C-L Wu, C R Praharaj and G K Khamari, *J. Phys.* **G25**, 501 (1999)
[3] P Quentin and H Flocard, *Ann. Rev. Nucl. Part. Sci.* **28**, 523 (1978)
[4] M Baranger and K Kumar, *Nucl. Phys.* **A110**, 410 (1968)
[5] I Y Lee *et al*, *Phys. Rev. Lett.* **39**, 682 (1974)
M V Hoen *et al*, *Phys. Rev.* **C24**, 1667 (1981)
F T Baker, *Nucl. Phys.* **A331**, 132 (1979)
[6] G D Alkhazov *et al*, *Nucl. Phys.* **A504**, 549 (1989)
C Thibault *et al*, *Nucl. Phys.* **A637**, 1 (1981)
[7] A Ansari, *Phys. Rev.* **C33**, 321 (1986)
[8] H Flocard, P Quentin and D Vautherin, *Phys. Lett.* **B46**, 304 (1973)
[9] T Cooper *et al*, *Phys. Rev.* **13**, 1083 (1976)
D Cline, *Ann. Rev. Nucl. Part. Sci.* **36**, 683 (1986)
[10] S K Patra, S Yoshida, N Takigawa, C R Praharaj and A K Rath, *Phys. Rev.* **C51**, 2248 (1995)
[11] S K Patra, Cheng-Li Wu, C R Praharaj and G K Khamari, *J. Phys.* **G25**, 501 (1999)
[12] S K Patra and C R Praharaj, *Phys. Rev.* **C44**, 2552 (1991)
[13] M Del Estal, M Centelles, X Viñas and S K Patra, *Phys. Rev.* **C63**, 024314 (2001)
[14] R Machleidt, *Adv. Nucl. Phys.* **19**, 189 (1989)
[15] Y K Gambhir, P Ring and A Thimet, *Ann. Phys.* **198**, 132 (1990)
[16] M Rufa, P-G Reinhard, W Greiner and M R Stranger, *Phys. Rev.* **C38**, 390 (1988)
P-G Reinhard, *Z. Phys.* **A329**, 257 (1993)
[17] C J Horowitz and B D Serot, *Nucl. Phys.* **A368**, 503 (1981)
[18] B D Serot and J D Walecka, *Adv. Nucl. Phys.* **16**, 1 (1986)
[19] G Ripka, *Adv. Nucl. Phys.* **1**, 1 (1966) edited by M Baranger and E Vogt (Plenum)
[20] C R Praharaj, *J. Phys.* **G14**, 843 (1988); *Phys. Lett.* **B119**, 17 (1982)
[21] A Faessler *et al*, *Phys. Rev.* **156**, 1067 (1967)
[22] P-G Reinhard, M Rufa, J Maruhn, W Greiner and J Friedrich, *Z. Phys.* **A323**, 13 (1986)
[23] P K Panda, S K Patra, J Reinhard and J Maruhn, *Int. J. Mod. Phys.* **E6**, 307 (1997)
[24] P Möller *et al*, *At. Data Nucl. Data Tables* **39**, 225 (1988)
D G Madland and J R Nix, *Nucl. Phys.* **A476**, 1 (1988)
[25] G A Lalazissis, J König and P Ring, *Phys. Rev.* **C55**, 540 (1997)
[26] M M Sharma, A R Farhan and S Mythili, *Phys. Rev.* **C61**, 054306 (2000)
[27] M Rashdan, *Phys. Rev.* **C63**, 044303 (2001)
[28] S Raman *et al*, *At. Data Nucl. Data Tables* **36**, 1 (1987)
[29] G Audi, O Berstllon, J Blachot and A H Webpstra, *Nucl. Phys.* **A624**, 1 (1997)
[30] S K Patra, B K Raj, M S Mehta and R K Gupta, *Phys. Rev.* **C65**, 054323 (2002)
[31] J L Wood, K Heyde, W Nazarewicz, M Huyse and P Van Duppen, *Phys. Rep.* **215**, 101 (1992)
[32] R Bengtsson and W Nazarewicz, *Z. Phys.* **A334**, 269 (1989)
[33] P Bonche, H Flocard, P-H Heenen, S J Krieger, and M S Weiss, *Nucl. Phys.* **A443**, 39 (1985)

[34] N Tajima, S Takahara and N Onishi, *Nucl. Phys.* **A603**, 23 (1996)
[35] S Takami, K Yabana and M Matsnu, *Phys. Lett.* **B431**, 242 (1998)
[36] M Yamagami, RIKEN Report No. 39 (September, 2001)
[37] W Koepf and P Ring, *Phys. Lett.* **B212**, 397 (1988)
[38] J Fink, V Blum, P-G Reinhard, J A Maruhn and W Greiner, *Phys. Lett.* **B218**, 277 (1989)
[39] D Hirata, H Toki, I Tanihata and P Ring, *Phys. Lett.* **B314**, 168 (1993)
[40] A Bohr and B R Mottelson, *Nuclear Structure* (W A Benjamin, New York, 1969) vol. I, ch. 2, p. 239
[41] M Hjorth-Jensen, T T S Kuo and E Osnes, *Phys. Rep.* **261**, 125 (1995)
[42] P Arumugam, Z Naik and S K Patra (in preparation)
[43] G F Bertsch, *Phys. Lett.* **B26**, 130 (1968)
[44] K Harada, *Phys. Lett.* **10**, 81 (1964)